PAPER *Special Section on Digital Signal Processing*

Image Contour Clustering by Vector Quantization on Multiscale Gradient Planes and Its Application to Image Coding

Makoto NAKASHIZUKA[†], *Member*, **Yuji HIURA**[††], *Student Member*, **Hisakazu KIKUCHI**[†††], *and* **Ikuo ISHII**[††], *Members*

SUMMARY We introduce an image contour clustering method based on a multiscale image representation and its application to image compression. Multiscale gradient planes are obtained from the mean squared sum of 2D wavelet transform of an image. The decay on the multiscale gradient planes across scales depends on the Lipshitz exponent. Since the Lipshitz exponent indicates the spatial differentiability of an image, the multiscale gradient planes represent smoothness or sharpness around edges on image contours. We apply vector quatization to the multiscale gradient planes at contours, and cluster the contours in terms of represntative vectors in VQ. Since the multiscale gradient planes indicate the Lipshitz exponents, the image contours are clustered according to its gradients and Lipshitz exponents. Moreover, we present an image recovery algorithm to the multiscale gradient planes, and we achieve the skech-based image compression by the vector quantization on the multiscale gradient planes.

key words: *sketch-based image coding, contour detection, image recovery, wavelet transform, multiscale analysis, vector quantization*

1. Introduction

Edge-based image coding [1]–[3] is one of the very low-bit rate image compression techniques. In the sketch-based image coding [1], an image is represented by image contours and intensity differences across the contours. Contour positions and qunatized intensity differences are recorded for image compression.

In decoding, an image is recovered by an iterative procedure. The recovery procedure minimizes a cost function which is defined by a constraint to the smoothness in intensity changes on planar regions [1]. The recovered image from the sketch-based image coding keeps only the intensity difference across the contours. Since the only information which is observed in the coded data is the intensity difference across the contours, all edges in the image are reconstructed in discontiniuous edges. The smoothness or sharpness of edges is lost in the image coding process.

The wavelet maxima representation [4]–[6] is employed as another approach to the image coding based on contours. If the wavelet maxima representation of which basic wavelet function corresponds to the first-order derivative of a smoothing function, the maxima indicate the positions of contours and describe a multiscale behavior of edges on contours. The entire set of wavelet maxima has enough information to reconstruct an original signal precisely. The wavelet maxima represent the original image as an edge representation over the several scales. The decay in maxima amplitude across scales depend on the Lipshitz exponents [4], [5], [7] of image edges. The Lipshitz exponent indicates the differentiability of the image intensity. Hence, the wavelet maxima representation is capable to represent the smoothness and sharpness in intensity changes on contours. In image coding by wavelet maxima [5], [6], only maxima which indicate contours around objects are selected by their multiscale behavior. The modulus of maxima along contours are recorded with a predictive coding.

In this paper, we introduce vector quantization [8] for a multiscale representation to cluster the image contours. The proposed clustering method is applied to a sketch-based image compression. Multiscale gradient planes are defined to describe image contours and are obtained from the squared sum of two dimensional wavelet transforms. The multiscale gradient planes allow us to describe the gradient of image intensity and the Lipshitz exponent on each image positions by its amplitude decay along scales. The vector quantization is applied to those vectors which consist of the multiscae gradients on several scales. These vectors on contours are replaced with representative vectors in a code-book of VQ. The contours are hence classified according to the representative vectors that indicate a multiscale behavior including the Lipshitz exponents.

For image compression, an image is coded in a form of the coarsest approximation image of the wavelet transform, contour positions and indices of the representative vectors. Not only the intensity gradient across contours but the information about differentiability of the edges on image contours are represented in the coded

Manuscript received December 10, 1997.
Manuscript revised March 5, 1998.

[†]The author is with the Graduate School of Bio-application and systems engineering, Tokyo University of Agriculture and Technology, Koganei-shi, 184–0012 Japan.
[††]The authors are with the Graduate School of Science and Technology, Niigata University, Niigata-shi, 950–2181 Japan.
[†††]The author is with the Faculty of Engineering, Niigata University, Niigata-shi 950–2181 Japan.

data. Hence smoothness and sharpness of the edges on contours can be recovered from the encoded images. In this paper, we demonstrate the possibility of the image coding by several representative vectors and evaluate the quality of recovered image. Also we would like to suggest a relationship between image quality and the number of the represetative vectors to demonstrate the advantage of the multiscale representation in sketch-based image coding.

In Sect. 2, we define the multiscale gradient planes by the dyadic wavelet transform. The multiscale properties of edges on image contours are explained by the decay of multiscale gradients across scales. In Sect. 3, The vector quantization is applied to the multiscale gradient planes for clustering image contours. Shape-gain vector quantization is employed to cluster image contours in terms of differentiability of edges. In Sect. 4, clustering results are applied to the sketch based image coding.

2. Multiscale Gradient Planes of Images

The one-dimensional dyadic wavelet transform [4]–[7] is defined as the convolution between a signal $f(x)$ and a wavelet function $\psi_j(x)$ as:

$$W_j f(x) = \psi_j * f(x) \tag{1}$$

where the wavelet fuction at j-th scale are derived from a basic wavelet $\psi(x)$ by scaling of 2^j as:

$$\psi_j(x) = \frac{1}{2^j}\psi\left(\frac{x}{2^j}\right) \tag{2}$$

where j is a positive integer and defines the scale of a wavelet function. The signal $f(x)$ is represented by the wavelet transforms $\{W_j f(x)\}_{j \in Z}$. In numerical computation, it is impossible to compute the value of a wavelet at an arbitrary fine scale and locations. Now, the finest scale j is assumed to be limited to one. The scaling function $\phi(x)$ is introduced to the scale limitation,

$$\phi_j(x) = \frac{1}{2^j}\phi\left(\frac{x}{2^j}\right) \tag{3}$$

and the smoothed function at j-th scale is computed by:

$$S_j f(x) = \phi_j * f(x). \tag{4}$$

The smoothed function $S_j f(x)$ is decomposed to the wavelet transform $W_{j+1}(x)$ and $S_{j+1}(x)$. $S_j f(x)$ is reconstructed with a synthesis wavelet function $\chi(x)$ that satisfies

$$|\Phi(\omega)|^2 = \sum_{j=1}^{+\infty} \Psi(2^j\omega)X(2^j\omega) \tag{5}$$

where $\Phi(\omega)$, $\Psi(\omega)$ and $X(\omega)$ indicate the Fourier transform of $\phi(x)$, $\psi(x)$ and $\chi(x)$, respectively. $S_j f(x)$ is now reconstructed by the fromula:

$$S_j f(x) = \chi_{j+1} * W_{j+1} f(x) + \phi^*_{j+1} * S_{j+1} f(x) \tag{6}$$

where $\phi^*_{j+1}(x)$ indicates $\phi_{j+1}(-x)$. Hence $S_1 f(x)$ which is the smoothed function of arbitrary function $f(x)$ is decomposed to the form of J-th scale smoothed function and a collection of the wavelet transforms as a sequence of functions

$$\{S_J f, \{W_j f\}_{1 \leq j \leq J}\} \tag{7}$$

where $S_j f$ and $W_j f$ denotes $S_J f(x)$ and $W_j f(x)$. In two dimensional case, a two dimensional smoothed function $S_j f(x,y)$

$$S_j f(x,y) = \phi_j * f(x,y) \tag{8}$$

is obtained by a two-dimensional convolution with a two-dimensional scaling function that is given by

$$\phi_j(x,y) = \phi_j(x)\phi_j(y). \tag{9}$$

In this paper, we define the two dimensional wavelet transform as

$$W_j^1 f(x,y) = \psi_j^1 * f(x,y) \tag{10}$$

and

$$W_j^2 f(x,y) = \psi_j^2 * f(x,y) \tag{11}$$

where two-dimensional wavelet functions are:

$$\psi_j^1(x,y) = \phi_{j-1}(x)\psi_j(y) \tag{12}$$

and

$$\psi_j^2(x,y) = \phi_{j-1}(y)\psi_j(x). \tag{13}$$

The smoothed image $S_1 f(x,y)$ is now represented in the form of the J-th scale smoothed image and two-directional components of the wavelet transforms

$$\{S_J f, (W_j^1 f)_{1 \leq j \leq J}, (W_j^2 f)_{1 \leq j \leq J}\}. \tag{14}$$

If the basic wavelet corresponds to the first-order derivative of a symmetric smoothing function $\theta(x)$, that is,

$$\psi(x) = \frac{d\theta(x)}{dx}, \tag{15}$$

then wavelet transforms, W_j^1 and W_j^2, can be written in the form of

$$\psi_j^1(x,y) = \frac{d\theta(2^{-j}y)}{dy}\phi_{j-1}(x) \tag{16}$$

and

$$\psi_j^2(x,y) = \frac{d\theta(2^{-j}x)}{dx}\phi_{j-1}(y). \tag{17}$$

Since the wavelet transforms approximate the first-order derivative of the j-th scale smoothed image, the root of the squared sum of two-directional wavelet transforms

$$M_j f(x,y) = \sqrt{(W_j^1 f(x,y))^2 + (W_j^2 f(x,y))^2} \tag{18}$$

approximates the gradient of j-th scale smoothed image. The surface defined by $M_j f(x,y)$ can be refered to as a multi-scale gradient plane. The ratio between $W_j^1(x,y)$ and $W_j^2(x,y)$ is lost in the multi-scale gradient planes. To get a complete image representation, the gradient direction planes described by

$$A_j f(x,y) = \tan^{-1} \frac{W_j^1 f(x,y)}{W_j^2 f(x,y)} \tag{19}$$

is defined. $S_1 f(x)$ can be represented as a collection of multi-scale gradient planes and gradient direction planes as

$$\{S_J f, (M_j f)_{1 \leqq j \leqq J}, (A_j f)_{1 \leqq j \leqq J}\}. \tag{20}$$

The multiscale behavior of $M_j f(x,y)$ is analyzed in terms of the Lipshitz exponent α [4]–[7] that satisfies

$$|f(x_0,y_0) - f(x_1,y_1)| \leqq C\sqrt{(x_0-x_1)^2 + (y_0-y_1)^2}^{\alpha}. \tag{21}$$

If there exists a constant, C around (x_0,y_0), α is refered to as the Lipshitz exponents. If $n < \alpha_0 < n+1$, then $f(x,y)$ is n times differentiable at (x_0,y_0). If a wavelet function is continuous and differentiable, then the multiscale gradients depend on the Lipshitz exponent as

$$M_j f(x,y) \leqq C(2^j)^{\alpha}. \tag{22}$$

Especially, the left hand side of (22) approximates to the right hand of (22) at the edegs on the image contours [4]. If the edge is discontinuous, then $\alpha = 0$ on the edge. On a smoother edge, α increases with diffirentiabilty of the edge.

The contour geometry in Fig. 1 (b) is detected by the maxima of the multiscale gradient at scale $j = 2$. The figure displays the positions where the amplitude of the multiscale gardient is greater than 1/8 of the maximum of the gradient plane at scale $j = 2$. Contours which represent the shape of objects in the image is well detected in the figure. The distribution of the multiscale gradient amplitude at contour positions displayed in Fig. 1 (b) is shown in Fig. 2, where, the relation of multiscale gradient between adjasent scales are plotted. There exist strong correlations between scales at the image contours.

An image can be approximated by the multiscale gradient planes which is sampled at the contour positions and can be recoverd by a coarse-to-fine recovery procedure [9]. The difference between given multiscale gradient planes and the gradient planes of a recovered image is decreased by a successive iteration of a coarse-to-fine recovery algorithm. The algorithm is briefly given in Appendix. A recovered image from the multiscale gradient planes and the coarsest component $S_3 f$ (Fig. 1 (c)) is shown in Fig. 1 (d). The texture and fine details which consist of the low-intensity changes are removed by a thresholding operation, but object

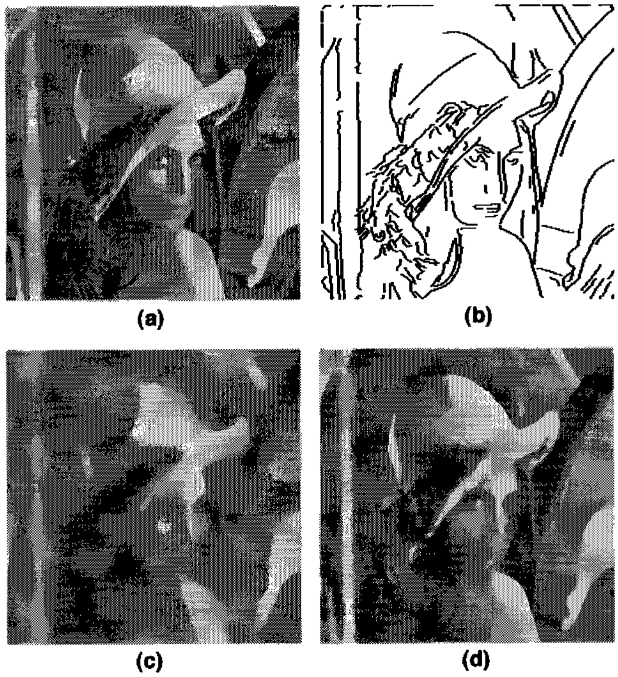

Fig. 1 (a) Original image, (b) contours detected from the wavelet maxima, (c) the coarsest approximation of (a), (b) recovered image from (c) and multiscale gradients of (b).

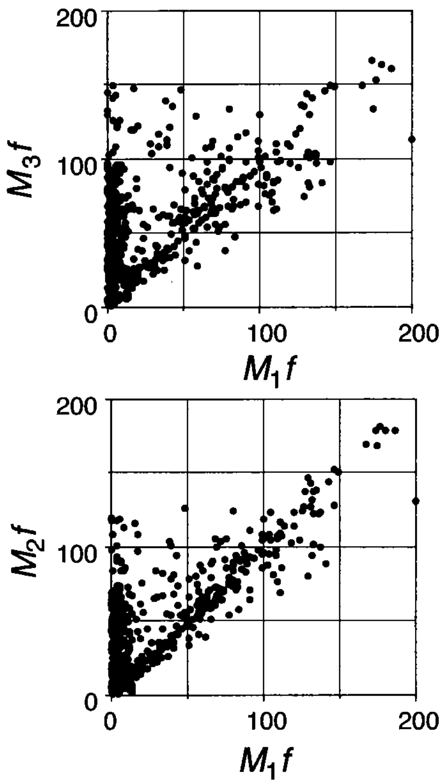

Fig. 2 Distribution of multiscale gradients on contours in Fig. 1 (b).

contours are still observed. Since multiscale gradient planes represent the Lipshitz exponents at contours, a recovered image keeps not only the intensity gradient but also the smoothness of intensity variation around contour positions.

3. Contour Clustering by Vector Quantization

Suppose that C is a set of significant contour positions, and

$$(x_c, y_c) \in C. \tag{23}$$

A multiscale gradient vector is defined by

$$\vec{v}(x_c, y_c) = [M_1 f(x_c, y_c), \ldots, M_J f(x_c, y_c)]^T \tag{24}$$

on every contour position (x_c, y_c).

After vector quantization is applied to the vector, we obtain the quantized vector

$$\vec{q}_k = Q[\vec{v}(x_c, y_c)] \tag{25}$$

where k indicates the vector index of representative vectors in a code book. Every vector is replaced with a closest representative vector in the code book. Contour positions (x_c, y_c) are classified in terms of representative vectors. Usually, a representative vector is selected to minimize the squared sum of quantization errors. For contour analysis with respect to Lipshitz exponents, we employ a shape-gain vector quatizer [8].

$\vec{v}(x_c, y_c)$ is split into two components: the gain factor

$$G(x_c, y_c) = \left(\sum_{j=1}^{J} (M_j f(x_c, y_c))^2 \right)^{1/2} \tag{26}$$

and the normalized shape vector

$$\vec{v^S}(x_c, y_c) = \left[\frac{M_1 f(x_c, y_c)}{G_1(x_c, y_c)}, \ldots, \frac{M_J f(x_c, y_c)}{G_J(x_c, y_c)} \right]^T. \tag{27}$$

Contour positions are hence separated into G and v^S. Ovbiously, the shape vector $\vec{v^S}(x_c, y_c)$ depends only on the ratio of multiscale gradient amplitudes along the scales. Contour positions are hence classified with respects to the Lpishitz exponent of the shape vector. The representative vector for $\vec{v^S}$ and the representative value for the gain $G(x_c, y_c)$are obtained by minmizing the squared sum of the quantization error [8]. As a result, every contour position is classified in terms of shape vectors and gains.

The clustering results for contour positions in Fig. 1 (b) are shown in Figs. 3 and 4. In this clustering, the number of the representative shape vectors is specified as 2 and the number of representative gains is specified as 4. Figure 3 displays four kinds of positions classified by the magnitude of gains as well as the classification result. Contours are simply classfied according to the intensity contrast across the contours. Positions of two representative shape vectors and clustering results are shown in Figs. 4 (a) and (b). Two bar graphs show the amplitude of each shape vector component. The amplitudes in Fig. 4 (a) are almost the same over three scales. This observation implies that Lipshitz exponents of the contour positions shown in Fig. 4 (a) is approximately equal to zero, and the contours of which edges are discontinuous are classified into this category.

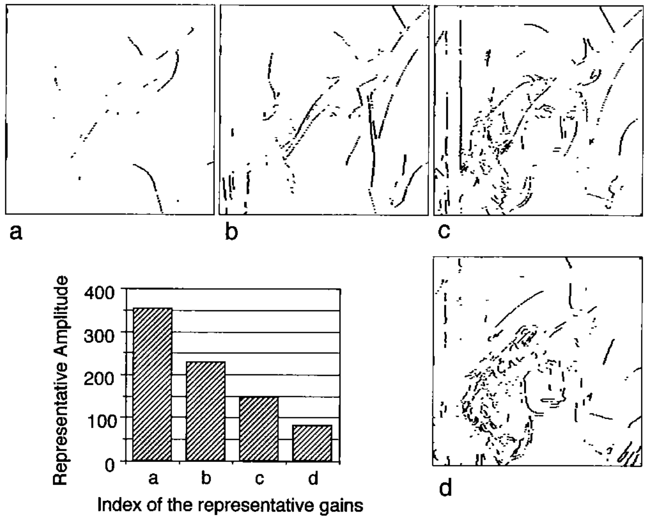

Fig. 3 Contour clustering by the gain of multiscale gradient vectors.

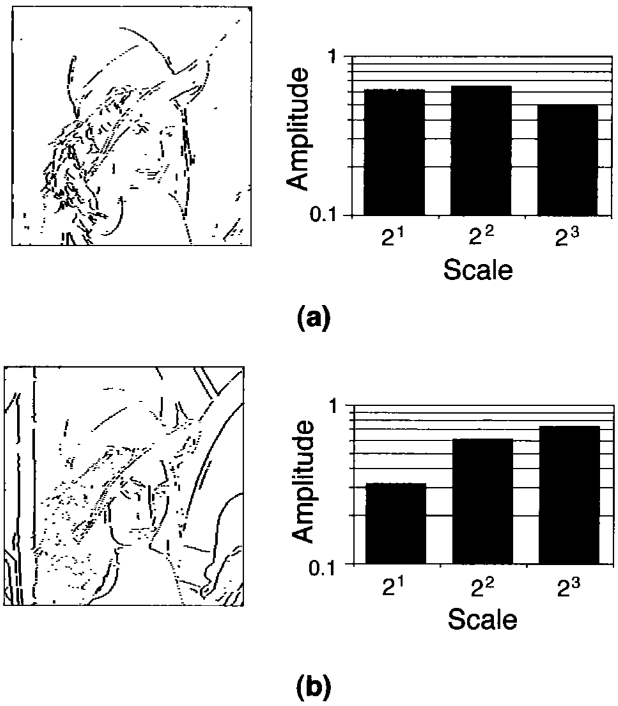

Fig. 4 Contour clustering by the shape of multiscale gradient vectors.

The most of contours around objects which exist on the camera focus are classified into the discontinuous conours as shown in Fig. 4 (a). In contrast, the contours in Fig. 4 (b) are classified in smoother edges. The amplitude of the representative shape vector decreases as the scale decreases. Lipshitz exponents of those contour positions shown in Fig. 4 (b) are larger than zero. These contours are smoother than those in Fig. 4 (a). The most of contours in the background and out-focusing regions are involved with Fig. 4 (b).

Next, we examine how many representative vectors are needed to approximate an original image. Now, we assume that the sum of the number of bits to represent the indices for gain and shape is constant. If N bits are allocated to a single contour position and n bits are allocated to represent the index of shape vectors, then the $N - n$ bits are spent for the index of representative gains. By this bit allocation, if the number of the representative shape in a code book is 2^n, then the number of the representative gains is 2^{N-n}. In Fig. 5, every connected plot belongs to the same bit budget given to a single contour pixel. The horizontal axis is measured in the bit budget for a representative shape vector.

Obviously, if the Lipshitz exponent can be approximated by a constant, none of bits is needed for the shape vector. As long as the total bit budget exeeds 2 bits per contour pixel, the best performance is obtained on $n = 1$. This means that just two kinds of representative shape vectors are found in the code book. Every contour is hence classified into one of two categories that are defined by whether the behavior of the Lipshitz exponent is constant or is decreasing.

A part of recovered images after the quantization is shown in Fig. 6. These images are recovered from the coarsest approximation and the multiscale gradient planes at the contour shown in Fig. 1 (b). Three bits are allocated to a single contour pixel for representing the multiscale gradient vector. All of contours that appear in the recovered image (b) from a single representative shape vector are approximated as discontinuous edges. In the image of (c), two kinds of shape vectors are used, and smoother edges are well recovered.

Our purpose in this section is the contour clustering in terms of Lipshitz exponents. The Lipshitz exponents are wll represented by the shape vector defined in Eq. (27), and hence we employ the shape-gain VQ. On the other hand, Fig. 7 shows the result of the conventional VQ with eight representative vectors. Comparing with Fig. 4, the shape-gain VQ clearly classifies contours in terms of smoothness of edges more than the conventional VQ. Obviously, the conventional VQ is superior to shape-gain VQ for reducing the quantization error. So, the conventional VQ will be more qualified for image coding and is applied to image coding in the next section. Coding result by the shape-gain VQ is also shown.

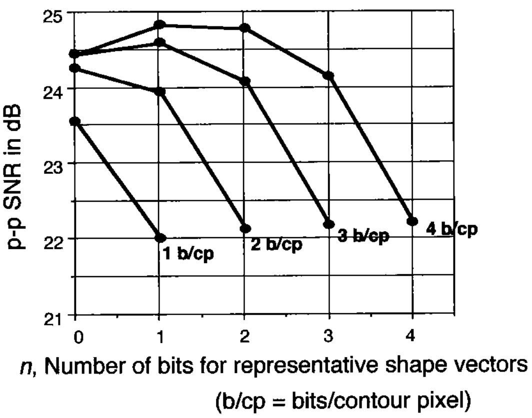

Fig. 5 Relation between the number of bits for a representative vector and the reconstruction precision.

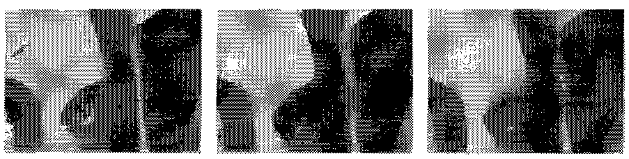

(a) **(b)** **(c)**

Fig. 6 (a) A part of the original image, (b) image recovered with a single representative shape vector, and (c) image recovered with two representative shape vectors.

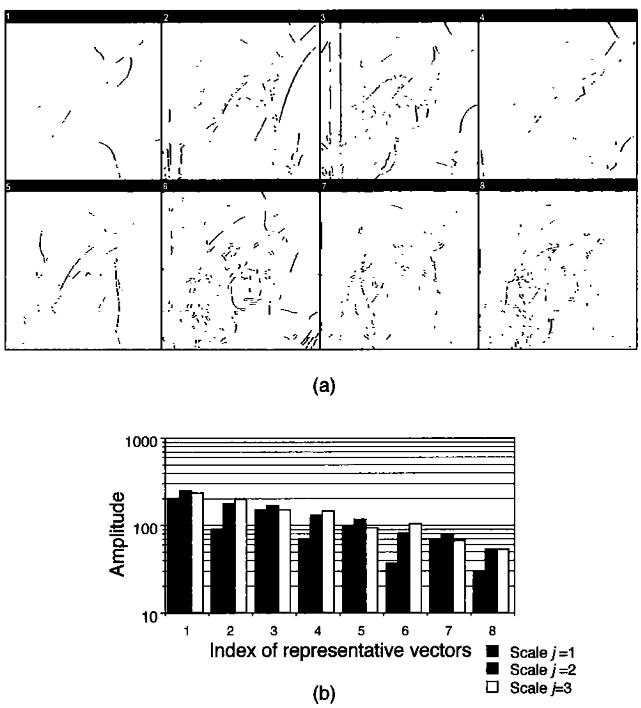

Fig. 7 (a) Contour clustering by the conventional vector quantization and (b) its representative vectors.

4. Application to Sketch-Based Image Coding

In this section, we apply the proposed contour clustering by VQ to sketch-based image coding. An image is going to be represented by three kinds of information: significant contour position C, the multiscale gradient vector $\overrightarrow{v}(x_c, y_c)$, and the coarsest approximation of the wavelet transform $S_J f$. The contour positions are encoded by a chain coding. Chains of contour positions are coded by recording the position of the first point of a chain and then coding the increments between two successive positions. In this coding, those successive are encoded by an entropy coding. The vector $\overrightarrow{v}(x_c, y_c)$ is quantized with a code book that is designed by the LBG algorithm to minimize the quantization error for each image. Hence every image is coded by its own different code book. Vector indexes are recorded along contours. Since the pixel intensity changes slowly along contours, just a single vector index that is dominant among consecutive three contour pixels is recorded.

A sequence of vector indexes are coded by run-length coding. The coarsest approximation $S_J f$ is down-sampled by 2^J and quantized into 6 bits. The quantized coarsest-approximation is encoded by a predictive coding with entropy coding.

To achieve high compression, contours that represent the shape of objects are selected. The contours are detected from the multiscale gradient maxima at scale $j = 2$ to avoid undesirable influences of maxima that occur because of textures and noises. Since Lipshitz exponent is positive values at image contours, the maxima points x, y where the multiscale gradient planes that satisfy

$$M_3 f(x, y) < M_2 f(x, y) \tag{28}$$

are removed. Moreover, to eliminate small details that is insignificant for human perception, we set the threshold on the basis of length and gradient to contours.

Figure 8 (a) is the reproduction with respect to the contour coding of Fig. 1 (a). The thresold for the contour length is set at 5. The threshold value for the gradient plane at sclae $j = 2$ is $1/8$ of the gradient maximum at scale $j = 2$. The contours of which length is shorter than 5 pixels or of which gradient amplitude is smaller than the threshold are removed. The maximum scale of the discrete dyadic wavelet transform is given as $J = 3$. The number of the representative vector in the code book is set to 8. Each component of the represetntaive vector is quantized to 8 bits. Since the multiscale gradients is obtained for 3 scales, the amount of code for the code book is 192 bits. Table 1 shows the amounts of coded data for the coarsest approximation, the contour positions, code-book and vector indexes. Almost half of the entire data is spent for the contour positions.

Figure 8 shows both the images coded by the proposed method and base-line JPEG images coded at the same data rate. Other examples are shown in Fig. 9 and Fig. 10. The coarse-to-fine recovery algorithm [9] is applied for decoding. All of those images cosist of 256-by-256 pixels. The error in encoded images and the total

(a) (b)

Fig. 8 (a) Image coded by the proposed method (0.28 bpp) and (b) image coded by JPEG.

Table 1 Data amount of code for each component in Fig. 8 (a).

Components	Amount of code (in bytes)
Coarsest approximation image	871
Contour positions	1049
Code-book of VQ	24
Vector Index allocated to each contour position	327

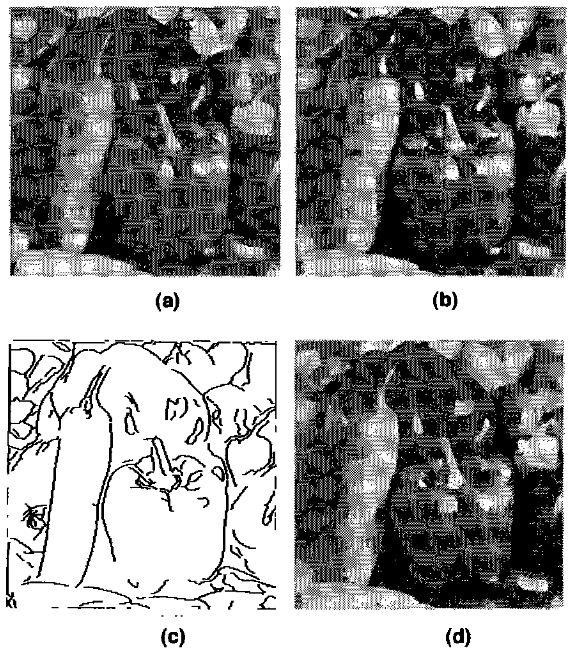

Fig. 9 (a) Original image, (b) JPEG coded image, (c) detected contours, and (d) image coded by the proposed method.

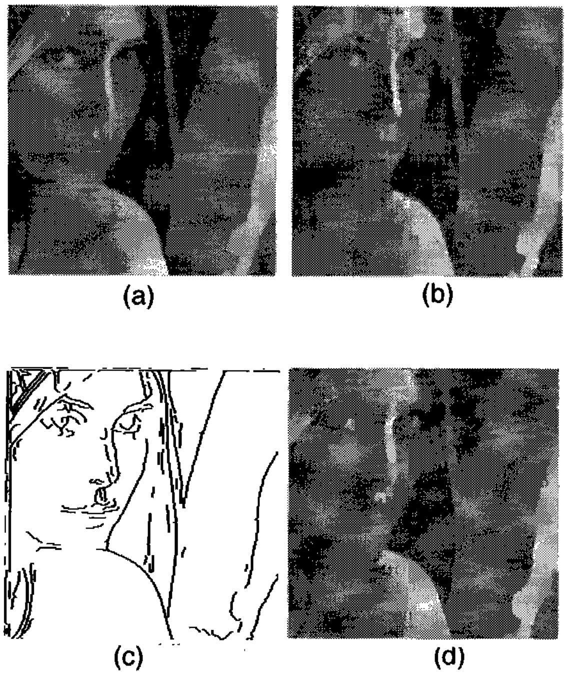

Fig. 10 (a) Original image, (b) JPEG coded image, (c) detected contours, and (d) image coded by the proposed method.

Table 2 Coding results for test images.

Image	Coder	Size in bytes	bits/pixel	Mean Absolute Error	Mean Squared Error	PSNR in dB
Fig. 8	Proposed	2,271	0.277	9.32	217.2	24.8
	Baseline JPEG	2,294	0.280	10.67	224.8	24.6
Fig. 9	Proposed	2,332	0.285	8.97	227.9	24.5
	Baseline JPEG	2,448	0.298	9.55	177.6	25.7
Fig. 10	Proposed	1, 762	0.215	4.77	51.4	31.4
	Baseline JPEG	1, 769	0.216	6.66	78.1	29.2

amount of coded data are shown in Table 2. We employ both MAE (Mean Absolute Error) and MSE (Mean Squared Error) to compare the proposed method with base-line JPEG. In all of images, the proposed method is superior to JPEG in MAE. However, MSE of JPEG is smaller than the proposed method in the coding example of Fig. 9. The reason to this is that the error that occurs in small regions with large amplitude is stressed than the error that occurs in large regions with small amplitude in MSE. Small details and textures are eliminated by the proposed method. Hence large parts of errors that occur in the encoded image concentrate to those parts of images. By contrast, the error in decoded images is spread over the whole image in JPEG. The lower parts in Fig. 8 also show a part of encoded images. Comparing with JPEG, image textures and small details have disappeared by the proposed method. However any distortions are not produced. Especially, the contour is well perceived in the decoded image. Moreover, the coding result of shape-gain VQ is shown in Fig. 11. The p-p SNR of the shape-gain VQ is slightly lower than the conventional VQ.

Fig. 11 Image coded by shape/gain vector quantization (0.294 dpp, p-p SNR 24.4 dB).

5. Conclusions

In this paper, we applied vector quantization to the multiscale gradient planes to the contour clustering in terms of the discontinuity of edges. The clustering method is applied to sketch-based image coding with a coarse-to-fine recovery algorithm. In contour clustering, the shape-gain vector quatinzation is applied. The contour is classified by its gradient and smoothness. The image recovery from various number of the representative vectors is demonstrated. The multiscale representation by the vector quantization can represent the smoothness of edges and is superior in SNR. In compression experiments by the conventional VQ for human facial images and still objects, eight representative vectors in a code book is enough for satisfactory recovery.

The compression results in our study are limited in extremely high compression ratios. Textures and fine structure of images are almost removed in the encoding process. By encoding the removed components, a layered image coding will be obtained. The proposed image coding could play a roll found in the layered image coding [10] by three components: the smoothed image, contours and textures. Such a layered image coding would be a qualified representation for the human perception and many other image processing tasks. Especially, contours are the primary information for pattern analysis, object recognition and scene analysis. The coded data that is obtained by the proposed image coding contains not only the contour positions but also information about intensity contrast and smoothness of edges on the contours. The information about image contours that is obtained by the proposed clustering method can be applied to computer vision applications.

References

[1] S. Carlsson, "Sketch based coding of gray level images," Signal Processing, 15, pp.57–83, 1988.
[2] M. Kunt, A. Ikonomopoulos, and M. Kocher, "Second-generation image-coding technique," Proc. IEEE, vol.73, no.4, pp.549–574, April 1985.
[3] M. Kunt, M. Benard, and R. Leonardi, "Recent results in high-compression imgae coding," IEEE Trans. Circuits & Syst., vol.34, no.11, pp.1306–1336, Nov. 1987.
[4] S. Mallat and W.L. Hwang, "Singularity detection and processing with wavelets," IEEE Trans. Inf. Theory, vol.38, no.2, pp.617–643, March 1992.
[5] S. Mallat and S. Zhong, "Characterization of signals from multiscale edges," IEEE Trans. Pattern Anal. & Mach. Intell., vol.14, no.7, pp.710–732, July 1992.
[6] J. Froment and S. Mallt, "Second generation compact image coding with wavelets," in "Wavelets: A tutorial in theory and applications," ed. C.K. Chui, Academic Press, 1992.
[7] G. Erlebacher, M.Y. Hussaini, and L.M. Jameson Eds., "WAVELETS Theory and Applications," Oxford University Press., New York, 1996.
[8] A. Gersho and R.M. Gray, "Vector Quantization and Signal Compression," Kluwer Academic Publisher, Massachusetts, 1992.
[9] M. Nakashizuka, H. Kikuchi, I. Ishii, and H. Makino, "A rotation insensitive multiscale image representation—definition and image recovery algorithm," IEICE Trans. Fundamentals, vol.J79-A, no.12, pp.2002–2013, Dec. 1996.
[10] X. Ran and N. Farvardin "A Perceptually motivated three component image model—part II: Applications to image compression," IEEE Trans. Image Processing, vol.4, no.4, pp.430–447, April 1995.

Appendix: Coarse-to-Fine Recovery Algorithm [9]

The coarse-to-fine recovery alogrithm recover the original image from the multiscale gradient. Let f be the original image and h be recovered image. The error of $M_j f$ and $S_J f$

$$D_h = \sum_{(m,n)\subset C} \left(\sum_{j=1}^{J} M_j h(m,n) - M_j f(m,n) \right)^2 + \sum_{n=0}^{N-1} \sum_{m=0}^{M-1} (S_J h(m,n) - S_J f(m,n))^2 \qquad (A\cdot 1)$$

is reduced along the course of recovery. To avoid the danger to be trapped into a local minimum, the minimization of the error begins from the coarsest approximation to the finest multiscale gradient. Suppose that $i = 0$, $k = 0$ and $j = J+1$. The following three-step operation is repeated L times on every scale, the initial image h^0 is given by $S_k f$

1. Compute the wavelet transform of h^i to get the form of (20).

2. If $j = J+1$ then replace $S_J h^i$ with $S_J f$ at the contour positions. If $j < J+1$ them replace $S_J h^i$ with $S_J f$ and replace $M_m h^i{}_{j\leq m\leq J}$ with $M_m f^i{}_{j\leq m\leq J}$ at the contour positions.

3. Increment i and k to $i+1$ and $k+1$ respectively. If $k = L$, then set k as zero and j as $j-1$. If $j = 0$, then stop the iteration. If $j > 0$, then compute $h^{(i+1)}$ by the inverse wavelet transform and go to 1.

Makoto Nakashizuka was born in Niigata, Japan, on January 31, 1966. He received B.E., M.E., and Ph.D. degrees from Niigata University, Niigata, Japan, in 1988, 1990, 1993. He was with Department of Information Engineering, Niigata University as a Research Associate from 1993 to 1997. He is now an Associate Professor at Graduate School of Bio-Applications and Systems Engineering, Tokyo University of Agriculture and Technology. His research interests include time-scale/frequency analysis and its applications to signal, bio-medical, vision and image processing. Dr. Nakashizuka is a member of IEEE, Japan Society of Medical Electronics and Biological Engineering and Institute of Image Information and Television Engineers.

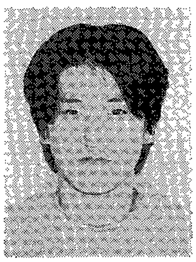

Yuji Hiura was born in Niigata, Japan, on July 29, 1974. He received B.E. degree from Niigata University, Niigata, Japan in 1996. He is now a master course student in Niigata university. His research interests include digital image processing and multiscale analysis.

Hisakazu Kikuchi was born in Niigata, Japan, on March 16, 1952. He received B.E. and M.E. degrees from Niigata University, Niigata, in 1974 and 1976, respectively, and Dr. Eng. degree in electrical and electronic engineering from Tokyo institute of Technology, Tokyo, in 1988. From 1976 to 1979 he worked at Information Processing Systems Laboratories, Fujitsu Ltd. Since 1979 he has been with Niigata University, where he is Professor in electrical engineering. During a year of 1992 to 1993, he was a visiting scientist at University of California, Los Angeles sponsored by the Ministry of Education, Science and Culture. His research interests include digital signal processing, image processing, wavelets, and mobile communication. Dr. Kikuchi is a member of IEEE and Japan SIAM.

Ikuo Ishii received the B.E. degree in electrical engineering from Niigata University, Niigata, Japan, in 1963, and the Ph.D. degree from Tokyo Institute of Technology, Tokyo, Japan. He is currently a professor at the Graduate School of Science and Technology, Niigata University. His current research interests are computer vision, image processing, and artificialintelligence. He is a member of the Information Processing Society of Japan and Japan Society of Medical Electronics and Biological Engineering.